OXFORD

ORIGINAL ARTICLE

Perceptual Training Restores Impaired Cortical Temporal Processing Due to Lead Exposure

Xiaoqing Zhu[1], Xia Liu[1], Fanfan Wei[1], Fang Wang[1], Michael M. Merzenich[3], Christoph E. Schreiner[3], Xinde Sun[1], and Xiaoming Zhou[1,2]

[1]Key Laboratory of Brain Functional Genomics of Ministry of Education, Shanghai Key Laboratory of Brain Functional Genomics, School of Life Sciences, East China Normal University, Shanghai 200062, China, [2]NYU-ECNU Institute of Brain and Cognitive Science at NYU Shanghai, Shanghai 200062, China, and [3]Coleman Memorial Laboratory, Keck Center for Integrative Neuroscience, University of California, San Francisco, CA 94143, USA

Address correspondence to Xiaoming Zhou. Email: xmzhou@bio.ecnu.edu.cn

Abstract

Low-level lead exposure is a risk factor for cognitive and learning disabilities in children and has been specifically associated with deficits in auditory temporal processing that impair aural language and reading abilities. Here, we show that rats exposed to low levels of lead in early life display a significant behavioral impairment in an auditory temporal rate discrimination task. Lead exposure also results in a degradation of the neuronal repetition-rate following capacity and response synchronization in primary auditory cortex. A modified go/no-go repetition-rate discrimination task applied in adult animals for ~50 days nearly restores to normal these lead-induced deficits in cortical temporal fidelity. Cortical expressions of parvalbumin, brain-derived neurotrophic factor, and NMDA receptor subunits NR2a and NR2b, which are down-regulated in lead-exposed animals, are also partially reversed with training. These studies in an animal model identify the primary auditory cortex as a novel target for low-level lead exposure and demonstrate that perceptual training can ameliorate lead-induced deficits in cortical discrimination between sound sequences.

Key words: low-level lead exposure, perceptual training, primary auditory cortex, processing deficits, rat

Introduction

Lead has long been known as a toxic agent with significant negative impacts on human neurological health. Despite extensive efforts to reduce the use of lead and to reduce environmental exposure, it continues to be a serious problem in many parts of the world, particularly the developing regions. The World Health Organization's (WHO's) current screening guidelines for preventing lead poisoning in young children consider a blood lead level of 10 µg/dL or higher to be of concern (WHO 1995). There is growing evidence, however, that blood lead levels even lower than this "toxic threshold" result in cognitive and learning disabilities of children including reading and language impairments (Lanphear et al. 2000; Canfield et al. 2003; Braun et al. 2006; Surkan et al. 2007; Zhang et al. 2013a,b; Grandjean and Landrigan 2014). Up

to this time, how low-level lead produces these negative changes in children remains largely unknown. However, it has been established that children with these behavioral syndromes also show deficits in auditory temporal processing and importantly, temporal processing abilities recorded in the auditory/aural speech sphere have been demonstrated, in normal individuals, to be generalized to other great sensory systems (Wright et al. 1997; Nagarajan et al. 1999; Ahissar et al. 2001; Fitch and Tallal 2003; Paterson et al. 2006; Fitch et al. 2013). All these findings thus indicate a disturbing relationship between low-level lead exposure, auditory temporal processing deficits, and behavioral dysfunction.

Earlier studies in animal models and humans have correlated low-level lead exposure with functional impairments in the central auditory system (Dietrich et al. 1992; Rothenberg et al. 2000;

Jones et al. 2008; Fortune and Lurie 2009; Prins et al. 2010). For example, it has been shown that lead exposure during development at blood levels of ~8.0 μg/dL alters normal monoaminergic expression in the mouse auditory brainstem (Fortune and Lurie 2009). Such exposure also decreases the expression of voltage-dependent anion channels and impairs temporal sound processing (i.e., gap detection) again recorded in the mouse midbrain (Jones et al. 2008; Prins et al. 2010). Adequate cortical processing of temporal fine-structures in environmental sounds and vocal communication signals is crucial for successful sound recognition and identification. The auditory cortex, as suggested by many behavioral, psychological, and physiological studies, plays a critical role in processing time-varying features of sound (Ahissar et al. 2001; Bowen et al. 2003; Rybalko et al. 2010). In humans, speech comprehension depends on response fidelity of cortical neurons to temporal envelopes of speech (Ahissar et al. 2001), and individuals with impaired language abilities and reading skills often demonstrate degraded temporal cortical responses (Wright et al. 1997; Nagarajan et al. 1999; Paterson et al. 2006). It is somewhat surprising, then, that it has not yet been determined how low-level lead exposure during development impacts temporal processing in the auditory cortex.

The current protocol of chelation therapy to reduce the blood lead level appears to be ineffective in remediating lead-induced neurodevelopmental deficits; these neurotoxic effects persist long after the blood lead level has returned to normal (Murphy and Regan 1999; Rogan et al. 2001; Lidsky and Schneider 2003; Bellinger 2008). Our earlier studies have shown that intensive perceptual training can refine developmentally degraded spectral tuning and temporal processing in the adult auditory cortex induced by an early disruption of the normal schedule of acoustic inputs (Zhou and Merzenich 2007, 2009). It is not known, however, whether or not a behavioral intervention strategy can restore a lead-induced auditory processing deficit.

Using the rat as an animal model, the current study was undertaken to determine whether low-level lead exposure during development impairs auditory cortical temporal processing and, if so, whether perceptual training can reverse these cortical deficits.

Materials and Methods

All procedures were approved by the Institutional Animal Care and Use Committee and complied with NIH standards.

Lead Exposure

Female offspring of timed-pregnant Sprague Dawley rats were used in these experiments. Offsprings were cross-fostered to achieve groups of 10 pups per litter at postnatal day 1 (p1) and were exposed to 58 mg/L lead acetate (Sigma) until p21, via their dams' drinking water. They were housed in a normal environment under an 8-h light/16-h dark cycle. After the weaning day (i.e., p21) pups were given free access to food and water containing no lead. Naïve rats were reared under identical housing conditions but were not exposed to lead. During experiments and analysis the researcher was held blind to the group identity of the animals.

Body weights of both mother and pups during lead exposure were continuously monitored, and were compared with that of age-matched naïve animals. No effects of exposure protocol on body weight gain were found for these lead-exposed rats, indicating normal lactation.

Blood Lead Levels

Lateral tail vein sampling was used for blood collection. Blood lead levels were measured by Graphite Furnace Atomic Absorption Spectrometry (GFAAS). Briefly, after diluted with a diluent/matrix modifier solution containing concentrated nitric acid, Triton X-100, and ammonium phosphate, the sample was loaded onto the GFAAS. A blood lead level was quantitated in comparison with external calibration solutions. Quality of the analytical run was controlled through the use of standard reference materials (SRMs) containing certified concentrations of the analyte (lead) and matrix matched blank samples.

Sound Discrimination Testing

Discrimination testing were conducted in an acoustically transparent operant training chamber (20 × 20 × 18 cm, length × width × height) enclosed within a sound-attenuated chamber. As described in earlier studies (Polley et al. 2006; Han et al. 2007; Zhou and Merzenich 2009), the rat's behavioral state was classified as either go or no-go. Rats were in the go state when the photobeam was interrupted by a nose-poke. All other states were considered no-go. Rats were rewarded for making a go response (a hit) within 3 s after target presentation; failure to respond within this time window was scored as a miss. A go response within 3 s of a nontarget stimulus was scored as a false positive, and the absence of response was scored as a withhold. The fifth state, false alarm, was defined as a go response that occurred 3 s or more after the stimulus presentation. A hit triggered the delivery of a 45-mg food pellet (BioServe). A miss, false positive, or false alarm initiated a 9 s time-out period, during which time house lights were turned off and no stimuli were presented. A withhold did not produce a reward or time out. An input and output system (photobeam detector, food dispenser, sound card, and house light; Med Associates) was used to control behavioral performance.

For sound temporal rate discrimination testing, rats were first trained to discriminate a 520-ms pulse train of 4 noise bursts (i.e., nontarget; repetition rate = 6.3 pulses per second, pps) from an 11-burst train of the same duration (target; repetition rate = 20 pps). Animals were returned to a normal housing environment after each day's training. When they reached steady performance scores after ~1 week of training, the temporal rate discrimination ability was tested by randomly delivering 520-ms nontarget pulse trains with pulse rates of 6.3, 8.3, 10, 12.5, or 14.3 pps, respectively. The target was always 20 pps during testing.

Trials were grouped into blocks of 50. At the conclusion of each block, a hit ratio (H; number of hits/number of target trials, expressed as a percentage) and a false positive ratio (F; number of false-positives/number of nontarget trials, expressed as a percentage) were calculated. Discrimination ability was quantified by a performance score, calculated as $H - F \times H$ (Han et al. 2007; Rybalko et al. 2010; Zhou and Merzenich 2012; Zhu et al. 2014).

Behavioral Training

To investigate effects of perceptual training on cortical temporal processing, lead-exposed rats were randomly divided into 2 groups: (1) trained rats, which were trained to identify a target auditory stimulus from a set of distractor stimuli to receive food rewards, for ~50 days. These auditory stimuli were pulse trains of same duration (520 ms) containing different numbers (5, 6, 7, 9, or 11) of noise bursts, corresponding to repetition rates of 8.3, 10, 12.5, 16.7, or 20 pps, respectively. (2) Sham rats, which were passively exposed to stimuli that were acoustically

and in stimulus quantity identical to that which were delivered to trained rats across the same epoch, but given free access to food.

Behavioral performance was shaped in 3 phases. Rats were initially pretrained to make a nose poke to obtain a food reward, and then trained to make a nose-poke response after presentation of a pulse train of 12.5 pps only. During the training stage, rats were conditioned to make a discriminative response to the target stimulus when a set of pulse trains of various repetition rates were randomly delivered; one of these pulse trains with a specific repetition rate was randomly chosen as the target, at the beginning of each day's training session. The input and output system used to control the behavioral performance was as described in the section of sound discrimination testing. An animal was considered well-trained if it achieved a performance score >80%, for 2 of the last 3 daily training blocks.

Auditory Brainstem Response (ABR) Measurement

ABR was measured in a shielded, double-walled sound chamber. Rats were anesthetized with an intraperitoneal injection of sodium pentobarbital (50 mg/kg body weight). Tone pips of 4, 8, 16, or 28 kHz at different intensities were delivered to the left ear through a calibrated earphone with a sound tube positioned inside the external auditory meatus. ABRs were recorded by placing silver wires subdermally at the scalp midline, posterior to the stimulated ear, and on the midline of the back 1–2 cm posterior to the neck. ABR signals were acquired, filtered, amplified, and analyzed using equipments and software (BioSig) manufactured by Tucker-Davis Technologies. The sound intensity that activated a minimal discernable response was defined as the ABR threshold.

Cortical Mapping and Data Analysis

Rats were anesthetized with sodium pentobarbital (50 mg/kg body weight). Throughout surgical procedures and during recording, a state of areflexia was maintained with supplemental doses of 8 mg/ml dilute pentobarbital injected i.p. Cortical responses were recorded with parylene-coated tungsten microelectrodes (1–2 megohms at 1 kHz; FHC). Recording sites were chosen to evenly sample from the auditory cortex while avoiding blood vessels, and were marked on a magnified digital image of the cortical surface vasculature. At each recording site the microelectrode was lowered orthogonally into the cortex to a depth of ~550 μm (layers IV–V) where evoked spikes of a neuron or a small cluster of neurons were recorded. Acoustic stimuli were generated and delivered to the contralateral ear relative to the recording site through a calibrated earphone with a sound tube positioned inside the external auditory meatus. A software package (SigCal, SigGen, and Brainware; Tucker-Davis Technologies) was used to calibrate the earphone, generate acoustic stimuli, monitor cortical response properties on-line, and store data for off-line analysis.

Frequency tuning curves of cortical neurons were reconstructed by presenting pure tones (25-ms duration) of 50 frequencies (1–30 kHz) at 8 sound intensities (0–70 dB SPL in 10 dB increments) in a random, interleaved sequence at a rate of 2 pps. The characteristic frequency (CF) of a cortical site was defined as the frequency at the tip of the V-shaped tuning curve. For flat-peaked tuning curves, characteristic frequency was defined as the midpoint of the plateau at threshold. For tuning curves with multiple peaks, characteristic frequency was defined as the frequency at the most sensitive tip (i.e., with lowest threshold). Response bandwidths 30 dB above threshold of tuning curves (BW30s) were measured for all sites.

To document cortical repetition rate transfer functions (RRTFs), trains of 6 tonal pulses (25-ms duration with 5 ms ramps at 60 dB SPL) were delivered 4 times at each of 8 repetition rates (2, 4, 7, 10, 12.5, 15, 17.5, and 20 pps) in a randomly interleaved sequence. The tone frequency was set at the CF of each site. To reduce variability resulting from different numbers of neurons included in different multiunit responses recorded, the normalized cortical response for each repetition rate was calculated as the average response to the last 5 pulses divided by the response to the first pulse (Kilgard and Merzenich 1998; Bao et al. 2004). The RRTF is the normalized cortical response as a function of the temporal rate of sound stimuli. The cortical ability for processing repetitive stimuli was estimated with the highest temporal rate at which the RRTF was at one-half its maximum ($f_{h1/2}$).

As previously described (Polley et al. 2006, 2007; Zhou and Merzenich 2009; Profant et al. 2013), the primary auditory cortex (A1) was identified based on the unique rostral-to-caudal tonotopy and reliable neuronal responses to tone pips of selective frequencies. The overall boundaries of A1 were functionally determined using nonresponsive sites and responsive sites that did not have well defined pure tone-evoked response areas (i.e., non-A1 sites; Zhou and Merzenich 2009). To generate A1 maps, Voronoi tessellation (a Matlab routine, The MathWorks) was performed to create tessellated polygons, with electrode penetration sites at their centers. Each polygon was assigned the characteristics (i.e., CF or $f_{h1/2}$) of the corresponding penetration site. In this way, every point on the surface of the auditory cortex was linked to the characteristics experimentally derived from a sampled cortical site that was closest to this point.

Misclassification rate (MR) was calculated by using the van Rossum spike train distance metric (van Rossum 2001) as described in our earlier studies (de Villers-Sidani et al. 2010; Zhou and Merzenich 2012). Each spike train was convolved with an exponential function, $N(t) = N_0 e^{-t/t}$, to obtain a filtered function. The distance between 2 spike trains was defined as the integral of the squared difference of 2 functions. Distances were calculated for all spike trains at a t of 10 ms in response to pulse trains of different rates. Confusion matrices were then constructed by calculating the average distance and s.d. between spike trains, with a misclassification recorded when the distance was less (for spike trains obtained with stimuli of dissimilar pulse rates) or more than (for spike trains obtained with stimuli of identical pulse rates) 1 s.d. away from the average distance.

The degree of synchronization between cortical sites was assessed by recording in silence for 10 periods of 10-s spontaneous neuronal spikes from 2–4 electrodes simultaneously. Cross-correlation functions were computed from each electrode pair by counting the number of spike coincidences for time lags of –50 to 50 ms with 1-ms bin size and were normalized by dividing each bin by the square root of the product of the number of discharges in both spike trains (Brosch and Schreiner 1999). Neural events occurring within 10 ms of each other in 2 channels were considered synchronous. For each pair of spike trains, we estimated the number of synchronized events if the 2 spike trains were not correlated, using $N_A N_B \Delta T$, where N_A and N_B are the number of spikes in the 2 spike trains, Δ (=21 ms) is the bin size, and T is the duration of the recording (Eggermont 1992; Bao et al. 2003). The strength of the synchrony was then assessed using a Z-score (Eggermont 1992):

$$Z = \frac{(\text{number of synchronized events} - N_A N_B \Delta/T)}{\sqrt{N_A N_B \Delta/T}}$$

For neural synchrony recording, offline spike sorting using TDT OpenSorter (Tucker-Davis Technologies) was carried out to include only single units in the analysis.

Immunohistochemistry

As in our earlier studies (de Villers-Sidani et al. 2010; Zhou and Merzenich 2012; Zhu et al. 2014), rats received a lethal dose of pentobarbital (85 mg/kg body weight) and were perfused intracardially with saline solution followed by 4% paraformaldehyde in 0.1 M potassium phosphate buffered saline (pH 7.2). Brains were removed and placed in the same fixative containing 20% sucrose for 12–24 h. Fixed material was cut in the coronal plane on a freezing microtome at 40-μm thickness. Free-floating sections were preincubated in a blocking solution to suppress nonspecific binding. The sections were then incubated at 4°C for 48–72 h in anti-parvalbumin (PV; Sigma), anti-brain-derived neurotrophic factor (BDNF; Millipore), or anti-NeuN (Millipore). After exposing to biotinylated IgG (Vector) at room temperature for 1 h, samples were treated further with streptavidin-conjugated Cy3 (Jackson ImmunoResearch) again at room temperature for 1 h.

Samples from different rat groups were always processed together during immunostaining procedures to limit variation related to antibody penetration, incubation time, and the postsectioning condition of the tissue. Fluorescence in the immunostained material was assessed and images were acquired (keeping exposure times constant for each series of tissue) using a Nikon E800 epifluorescent microscope equipped with a camera (AxioCam, Zeiss). A neuron was counted only if the staining revealed a complete soma perimeter and the neuron was clearly differentiated from background.

Quantitative Immunoblots

After rats were anesthetized with sodium pentobarbital (50 mg/kg body weight), the overall boundaries of the A1 were functionally determined using electrophysiological recording procedures as described above. Animals then were deeply anesthetized with an additional dose of sodium pentobarbital (35 mg/kg body weight). The A1 was rapidly dissected, frozen in dry ice, and stored at −80°C until processing.

Quantitative immunoblotting was performed as described previously (Cai et al. 2010; Zhou et al. 2011; Guo et al. 2012; Zhang et al. 2013a,b) with slight modifications. Briefly, equal amounts of synaptoneurosomal proteins, determined using the bicinchoninic acid assay, were resolved in 7.5% sodium dodecyl sulfate-polyacrylamide gels and then transferred to nitrocellulose membranes. After both primary and secondary antibody incubations, immunoreactive bands were visualized using a Bio-Rad Universal Hood 2 imaging system (Bio-Rad). Primary antibodies included anti-NMDA NR2a and NR2b (Millipore), and anti-β-actin (Millipore).

The density of each band on Western blotting was measured and the relative level of each protein was calculated as a ratio against β-actin, normalized to that of naïve control.

Results

Blood Lead Levels

Rat pups were exposed to 58 mg/L lead acetate from p1 to p21 delivered via their dams' drinking water. After the weaning day (i.e., p21) the pups had direct access to drinking water containing no lead (Fig. 1A). This exposure protocol resulted in blood lead levels of 7.9 ± 0.1 μg/dL measured at p9 and 8.2 ± 0.1 μg/dL at p21.
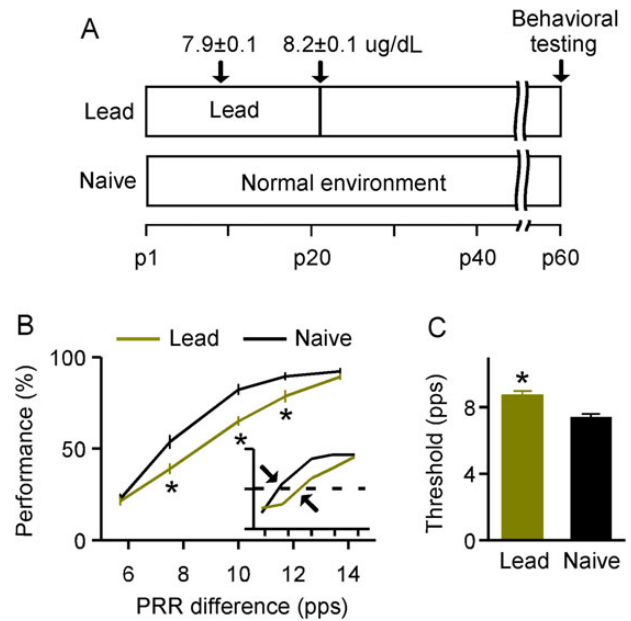

Figure 1. Deficits in sound temporal rate discrimination tasks induced by lead exposure. (A) Experimental timelines for lead-exposed and naïve rats. Mean values (μg/dL) measured at 2 specific postnatal days for lead-exposed animals (i.e., p9 and p21; $N = 35$) are also shown. Note that no lead was detected in naïve animals when measured at p9 and p40. (B) Average psychometric curves obtained from lead-exposed ($N = 15$) and naïve ($N = 17$) rats. Inset shows examples of psychometric curves. Dashed line and arrow show 50% of maximal score and the discrimination threshold for each psychometric curve, respectively. PRR, pulse repetition rate. Error bars represent SEM. $^*P < 0.005$. (C) Comparison of discrimination thresholds for lead-exposed and naïve rats. $^*P < 0.0001$.

Thereafter, the blood lead level decreased, with no lead detectable at p40. In naïve animals, no lead was detected when measured at p9 and p40, respectively.

Deficits in Auditory Temporal Rate Discrimination

We first evaluated the possible consequence of lead exposure on sound-elicited temporal rate discrimination performance for lead-exposed versus naïve rats at ~p60 (Fig. 1A). Rats were initially trained to discriminate between pulse trains presented at 6.3 pps (the "nontarget") and 20 pps (the "target"). The detection of this large difference in the temporal rate of presented pulse trains (i.e., 6.3 vs. 20 pps) was perceptually unchallenging; both lead-exposed and naïve rats achieved steady performance scores (>80%) after ~1 week of training. On the following day, all animals with identical training histories underwent a testing phase in which the nontarget for each trial was randomly chosen from pulse trains varying in repetition rate (i.e., 6.3, 8.3, 10, 12.5, or 14.3 pps), while the target was always 20 pps. A psychometric curve then was obtained by plotting the performance score as a function of the rate difference between the target and the nontarget, to estimate the temporal rate discrimination ability for each animal. As shown in Figure 1B, while performance scores for both rat groups increased with larger rate differences, all values at intermediate rate differences were significantly lower for lead-exposed than for naïve rats (2-way ANOVA with Student–Newman–Keuls post hoc test, all $P < 0.005$). It should be noted that both groups showed high performance scores at a rate difference of 14.3 pps (2-way ANOVA with Student–Newman–Keuls post hoc test, $P = 0.44$) as it was perceptually unchallenging for these rats

to discriminate such large differences between the target and the nontarget. They also had similar performance scores at a rate difference of 6.3 pps (2-way ANOVA with Student–Newman–Keuls post hoc test, $P = 0.76$) probably because this difference was too small to be discriminated and they all responded by chance. As expected, discrimination thresholds (defined as the rate difference corresponding to a 50% performance score on the psychometric curve; Fig. 1B, inset), were significantly higher in lead-exposed than in naïve rats (Fig. 1C; unpaired t-test, $P < 0.0001$). These results indicate a decreased ability to discriminate between rates of temporally modulated sound after lead exposure.

Postexposure Alterations in Cortical Temporal Responses

We next examined cortical responses of lead-exposed versus naïve rats, using conventional extracellular unit recording techniques again at ~p60 (see Fig. 1A for experimental timelines). Data were recorded from neurons in A1 from 244 sites in 5 naïve rats and from 288 sites in 6 lead-exposed rats. Unless otherwise specified, all subsequent quantitative analyses in this section are based on these samples. As previously described (Polley et al. 2006, 2007; Profant et al. 2013), A1 has a unique rostral-to-caudal tonotopy and reliable neuronal responses to tone pips of selective frequencies (Supplementary Fig. 1A and B). The distributions of CFs for recorded cortical sites did not differ between 2 groups of rats (Supplementary Fig. 1C; Kolmogorov–Smirnov test, $P = 0.33$).

Figure 2A shows examples of cortical responses to tonal pulses at the CF delivered at variable repetition rates. While cortical neurons in naïve rats could follow repeated stimuli at and below rates of 10 pps, neurons in lead-exposed rats could only follow stimuli at or below 7 pps (Fig. 2A; lead vs. naïve). As shown by the RRTFs in which normalized cortical responses were defined as a function of stimulus repetition rates (Fig. 2A insets, and Fig. 2B), neurons in lead-exposed rats displayed a decreased modulation of their responses at rates of 4–20 pps, compared with naïve rats (Fig. 2B; 2-way ANOVA with Student–Newman–Keuls post hoc test, $P < 0.05$–0.001). We quantified the cortical capacity for processing the high-rate stimuli by determining the highest rate at which RRTF was at half of its maximum (i.e., $f_{h1/2}$; Fig. 2A, arrows in insets). As shown in Figure 2C which illustrates representative cortical $f_{h1/2}$ maps for both rat groups, $f_{h1/2}$s obtained at most cortical sites were lower in lead-exposed than in naïve rats (Fig. 2C, left vs. right). A comparison of distributions for $f_{h1/2}$s also showed a significant decrease (leftward shift) for lead-exposed versus naïve rats (Fig. 2D; Kolmogorov–Smirnov test, $P < 0.001$), demonstrating a decreased rate-following ability induced by lead exposure. This degradation was consistent for neurons across all CF ranges (Fig. 2E; 2-way ANOVA with Student–Newman–Keuls post hoc test, $P < 0.01$–0.001).
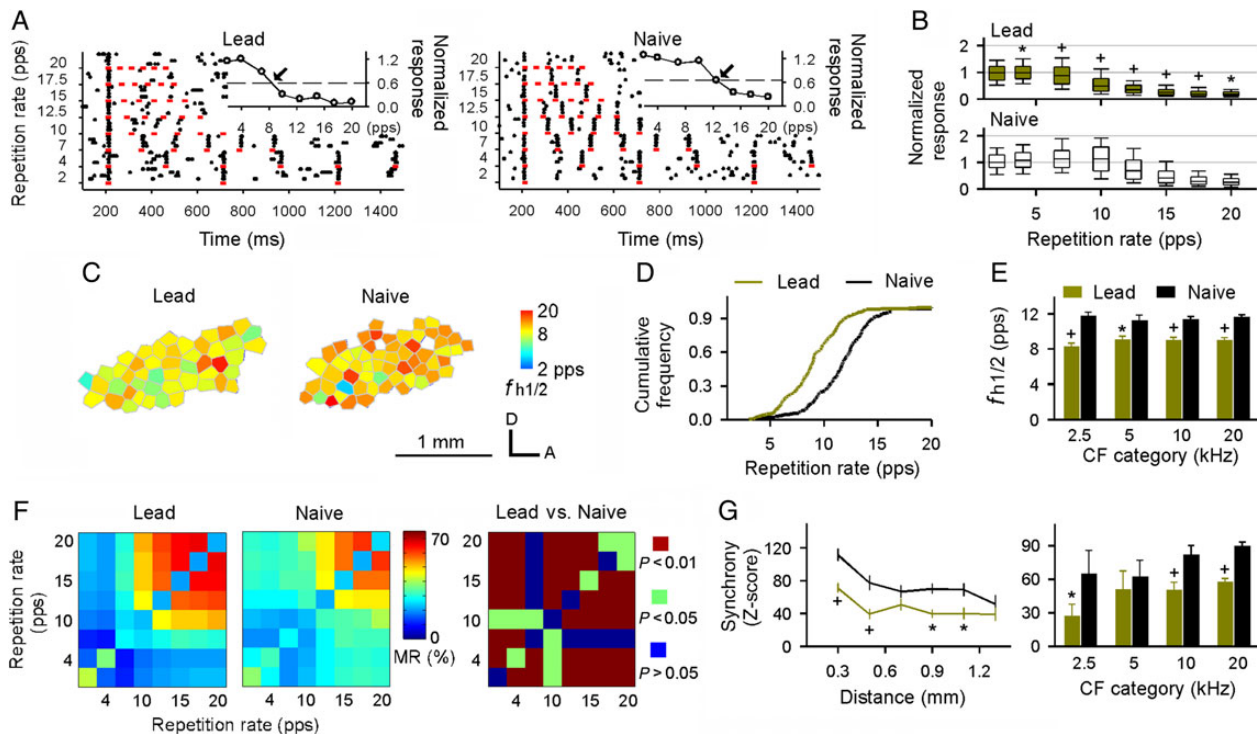

Figure 2. Postexposure changes in cortical temporal responses. (A) Dot raster plot examples showing cortical responses to pulse trains of different repetition rates recorded from lead-exposed (left) and naïve (right) rats. Red lines indicate pulse durations. Inset shows the RRTF for each raster plot example. Dashed line and arrow show 50% of maximal normalized response and $f_{h1/2}$ for each RRTF, respectively. (B) Normalized responses for all recordings against stimulus repetition rates obtained from lead-exposed (top) and naïve (bottom) rats. Graphs plot the median, 10th, 25th, 75th, and 90th percentiles as vertical boxes with error bars. * or +, $P < 0.05$ or 0.001. (C) Representative auditory cortical $f_{h1/2}$ maps for lead-exposed and naïve rats. The color of each polygon indicates the $f_{h1/2}$ recorded at that site. Unfilled polygon indicates that the RRTF was not recorded at the site. D, dorsal; A, anterior. (D) Cumulative frequency histograms showing a significant leftward shift of the $f_{h1/2}$ distribution for lead-exposed compared with naïve rats. (E) Average $f_{h1/2}$s for all recording sites in lead-exposed and naïve rats, for each of 4 CF ranges. Error bars represent SEM. Bin size = 1 octave. * or +, $P < 0.01$ or 0.001. (F) Average MRs for lead-exposed and naïve rats (left and middle) and results of t-test for comparisons between lead-exposed and naïve rats (right). (G) Average Z-scores of firing synchrony as a function of distance between 2 cortical recording sites (left) and Z-scores across A1 regions representing different frequency categories (right). * or +, $P < 0.05$ or 0.001.

To examine the reliability of cortical temporal responses to repetitive stimuli, we calculated the misclassification rate for every possible combination of pulse trains by using the Van Rossum spike train distance metric (van Rossum 2001; de Villers-Sidani et al. 2010; Zhou and Merzenich 2012; see also Materials and Methods). MR quantifies the similarity between spike trains recorded using different pulse trains, or the difference between spike trains recorded using identical pulse trains while taking into account the spike number and timing. Smaller MR values therefore indicate more reliable spike trains representing temporal structure of pulse trains. As shown in Figure 2F, the average MRs for combinations of dissimilar high pulse rates (i.e., 10–20 pps) were significantly larger in lead-exposed versus naïve rats (see P values in Fig. 2F, right), indicating more confusable responses to repetitive stimuli as a result of lead exposure. It is interesting to note that the MR values for some combinations of low and high rates for lead-exposed rats were also smaller than naïve rats.

Neural synchrony in A1 was documented by simultaneously recording spontaneous firing from cortical sites separated by variable distances, to assess horizontal cortical network connectivity (Brosch and Schreiner 1999; Bao et al. 2003; Zhou et al. 2011). While spontaneous firing rates recorded from the 2 groups of rats were comparable (8.0 ± 0.38 spikes/s for lead-exposed rats and 8.8 ± 0.35 spikes/s for naïve rats; unpaired t-test, $P = 0.13$), the average correlation strengths normalized for firing rates between −10 and 10 ms lags were 17.8% less for lead-exposed than for naïve rats (unpaired t-test, $P < 0.00001$), indicating weaker cortical network coupling due to lead exposure. We quantified the strength of discharge synchrony between cortical sites that were recorded simultaneously in A1 by using a Z-score (Eggermont 1992; see also Materials and Methods). The Z-score value is the observed frequency of synchronized events in 2 neurons corrected for what would be expected by chance alone. As shown on left of Figure 2G, Z-scores for pairs of simultaneously recorded cortical sites in both groups decreased as a function of inter-electrode distances. However, values were lower at all electrode separations in lead-exposed than in naïve rats with statistical significance at separations of 0.3, 0.5, 0.9, and 0.11 mm (2-way ANOVA with Student–Newman–Keuls post hoc test, $P < 0.05$–0.001). Induced changes applied for cortical zones representing low-to-high frequencies (Fig. 2G, right; 2-way ANOVA with Student–Newman–Keuls post hoc test, $P < 0.05$–0.001 except for CF category of 5 kHz where $P > 0.05$).

We further evaluated the cortical frequency selectivity by constructing frequency tuning curves then measured their bandwidths 30 dB above the threshold (i.e., BW30s). As shown in Supplementary Figure 2A, the average BW30 recorded from lead-exposed rats was slightly larger than that of naïve rats at each CF category, but differences did not reach statistical significance (2-way ANOVA, $P = 0.12$). In addition, cortical response thresholds were comparable for the 2 groups (Supplementary Fig. 2B; 2-way ANOVA, $P = 0.62$). These repeated measures of unit response thresholds combined with ABR measurements (Supplementary Fig. 3) show that low-level lead exposure has no measurable impact on hearing thresholds per se.

Perceptual Training Restores Degraded Cortical Temporal Responses

Our next goal was to determine whether perceptual training strategies could restore lead-induced deficits in cortical temporal processing. Beginning at p60, lead-exposed rats were trained over a period of ~50 days to identify a target auditory stimulus (pulse

train of a specific repetition rate) that was presented against a background of varying nontarget auditory stimuli (pulse trains of variable repetition rate) to receive food rewards. The repetition rate of the target pulse train changed daily on a random schedule. On early training days, these rats continuously nose-poked on each trial to receive food rewards, resulting in high-response rates for both targets and nontargets (Fig. 3A, left). Performance scores thus were always low with nose-pokes in each block distributed almost equally over all pulse trains presented (Fig. 3B, left; one-way ANOVA, $P = 0.08$–0.28 except for block 5 where $P = 0.003$).

As training progressed, however, rats learned to identify and selectively respond to the new, randomly set target pulse train on each training day. They still nose-poked continuously during each training day's initial block, shown by high rates of both target and nontarget responses and a low performance score (first block in Fig. 3A, right). Starting from the second block, however, rats began to master the behavior and consolidate their identification of the target, and nontarget responses sharply declined (one-way ANOVA with Student–Newman–Keuls post hoc test, all $P < 0.001$ compared with the first block) while target-response rates remained high (one-way ANOVA, $P = 0.18$). Performance scores thus significantly increased (one-way ANOVA with Student–Newman–Keuls post hoc test, all $P < 0.001$ compared with the first block), with nose-pokes for these blocks consistently sharply favoring the new (for that day) target (Fig. 3B, right; one-way ANOVA with Student–Newman–Keuls post hoc test, all $P < 0.001$).

Cortical temporal responses of these lead-exposed-then-trained rats were documented in detail at the end of training (at ~p110, Fig. 3C; recording sites = 214 from 5 rats). Data were compared with those recorded from sham (recording sites = 282 from 6 rats) and naïve rats (recording sites = 399 from 8 rats).

RRTFs were derived to characterize cortical temporal responses for the different groups. As shown in Figure 3D, cortical responses in sham rats fell off rapidly above 7 pps compared with naïve rats (2-way ANOVA with Student–Newman–Keuls post hoc test, all $P < 0.001$). Cortical responses for trained rats increased significantly at these repetition rates (i.e., 7–15 pps) compared with sham rats (2-way ANOVA with Student–Newman–Keuls post hoc test, all $P < 0.001$) and were now comparable with those recorded in naïve rats (2-way ANOVA with Student–Newman–Keuls post hoc test, all $P > 0.25$). As expected, while average $f_{h1/2}$s were lower for sham compared with naïve rats (2-way ANOVA with Student–Newman–Keuls post hoc test, all $P < 0.001$ except for CF category of 5 kHz where $P = 0.086$; Fig. 3E), $f_{h1/2}$s for trained rats were not different from naïve rats across all CF categories (2-way ANOVA with Student–Newman–Keuls post hoc test, all $P > 0.36$).

We also compared MRs for combination of pulse trains used to construct the RRTFs for different rat groups. As shown in Figure 3F, MRs of sham rats for some combinations of dissimilar high pulse rates (i.e., 10–20 pps) were significantly larger compared with control rats (denoted with asterisks in Fig. 3F, middle; all $P < 0.05$–0.01). Sound rate discrimination training reduced the MRs such that values for trained rats were comparable with, or even smaller than those for naïve rats (denoted with crosses in Fig. 3F, top; all $P < 0.05$–0.01). These results indicate that a decreased reliability of cortical temporal responses to repetitive stimuli in sham rats is partially revered as a result of discrimination training.

We again used pair-wise recording of spontaneous activity to compare neural synchrony in cortical field A1 for different groups (Fig. 3G). The average Z-scores for pairs of simultaneously
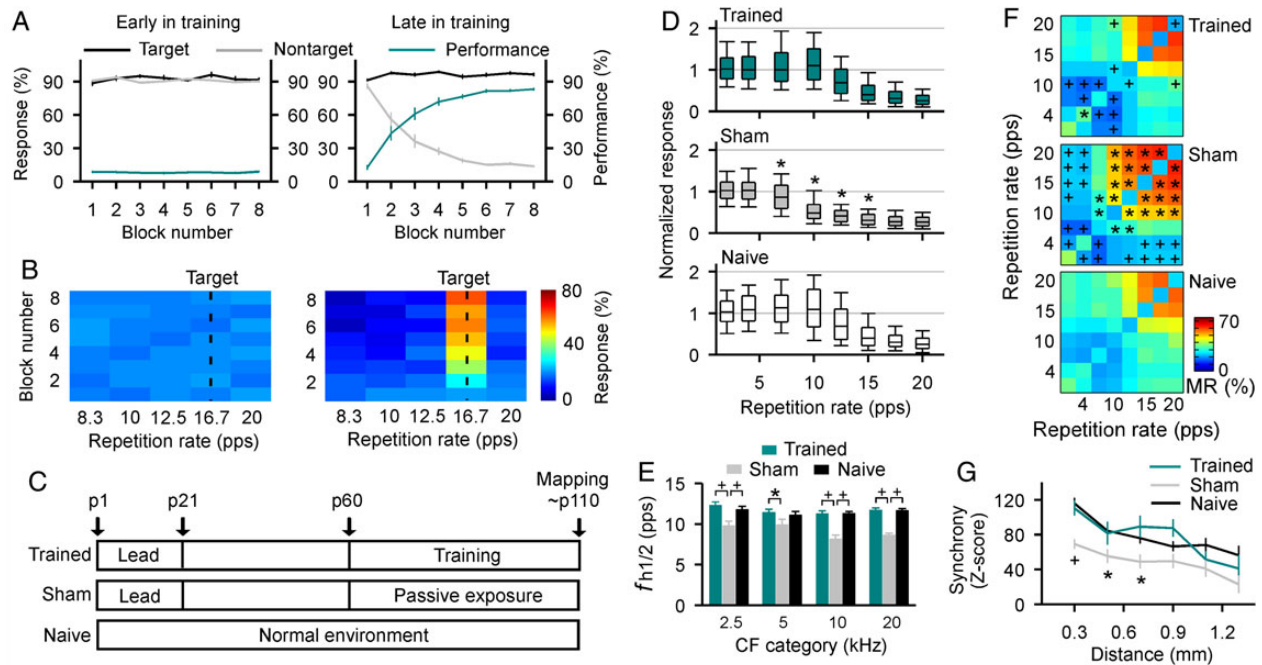
Figure 3. Degraded cortical temporal responses restored by intensive training. (A) Target and nontarget responses for each block during a single training day while learning a temporal rate discrimination task for lead-exposed rats (N = 8) in the early (left) or late (right) training phase. Note that these rats were trained for ~50 days, beginning at p60, to identify a target auditory stimulus presented with varying nontarget auditory stimuli, to receive food rewards. The performance score for each block is also shown (right ordinate). Error bars represent SEM. (B) Distribution of total responses for each block. Values shown are mean values of all animals. Dashed lines indicate target stimuli. (C) Experimental timelines for different groups. Note that sham rats were exposed passively to stimuli identical to those that were delivered to trained rats across the same epoch but were given free access to food. (D) Normalized cortical responses to repetitive stimuli of different PRRs recorded from different groups. Graphs plot the median, 10th, 25th, 75th, and 90th percentiles as vertical boxes with error bars. Note that statistical analysis showed that normalized responses recorded from naïve rats at ~p110 (155 sites from 3 rats) were not different from that recorded at ~p60 (244 sites from 5 rats; 2-way ANOVA, P = 0.63). These data therefore were combined as naïve data here to minimize the number of animals used in the study. *P < 0.001 compared with naïve or trained rats. (E) Average $f_{h1/2}$s for all recording sites in different groups. * or +, P < 0.05 or 0.001. (F) Average MRs for different groups. * or +, MRs were significantly larger or smaller compared with naïve rats (one-way ANOVA with post hoc Student–Newman–Keuls tests, P < 0.05–0.01). (G) Average Z-scores of neuronal firing synchrony as a function of distance between 2 recording sites for different groups. * or +, P < 0.05 or 0.001 compared with naïve or trained rats.
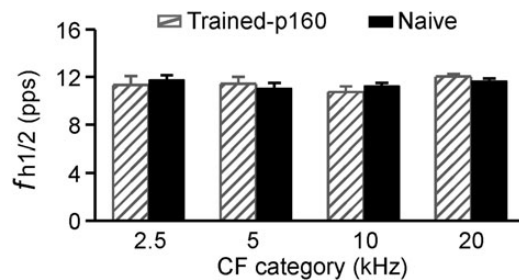

Figure 4. Average $f_{h1/2}$s values of trained rats measured at approximately p160 (i.e., ~50 days after the end of training; recording sites = 195 from 4 rats), illustrated with naïve rats. Error bars represent SEM.

recorded cortical sites in trained rats were similar to naïve animals (2-way ANOVA with Student–Newman–Keuls post hoc test, all P > 0.14). In contrast, sham rats showed lower neural synchrony compared with naïve animals at all electrode separations (2-way ANOVA with Student–Newman–Keuls post hoc test, P < 0.05–0.001 at separations ranging from 0.3 to 0.7 mm).

To evaluate enduring effects of perceptual training on temporal cortical responses, 4 trained rats were returned to a standard housing condition with RRTFs constructed at approximately p160 (i.e., ~50 days after the end of training). As shown in Figure 4, $f_{h1/2}$ values recorded at p160 were still comparable with those of

naïve rats (2-way ANOVA, P > 0.8), indicating that training-induced reversal of cortical rate-following ability endured for at least 50 days after training cessation.

Training-Induced Reversal of Cortical Molecular Changes

To document cellular and molecular changes at cortical level impacted by lead exposure and their potential restoration to normal values by training, we first quantified the expression levels of PV and BDNF, both proposed to contribute to the regulation of cortical plasticity (de Villers-Sidani et al. 2008; Maya Vetencourt et al. 2008; Baroncelli et al. 2010; Zhou and Merzenich 2012; Singer et al. 2014; Zhu et al. 2014). More specifically, cortical PV+ neurons have been shown to regulate the temporal precision of cortical responses rather than shape their frequency tuning (Moore and Wehr 2013). We found significant differences in numbers of PV-immunostained (PV+) neurons across cortical layers II/III–VI (2-way ANOVA, P < 0.001) and among the 3 groups (P < 0.001). A Student–Newman–Keuls post hoc test confirmed that the numbers of PV+ neurons in sham rats were lower than in naïve rats across cortical layers II/III–VI (P < 0.05–0.001; Fig. 5B vs. C, and D). Reduced dentritic PV immunoreactivity was also noted in sham compared with naïve rats (Fig. 5B vs. C). Perceptual training partially reversed these differences; the numbers of PV+ neurons in trained rats were no longer significantly different from that of naïve rats in cortical layers II/III, V, and VI (2-way ANOVA with Student–Newman–Keuls post hoc test, all P > 0.05; Fig. 5A vs. C,
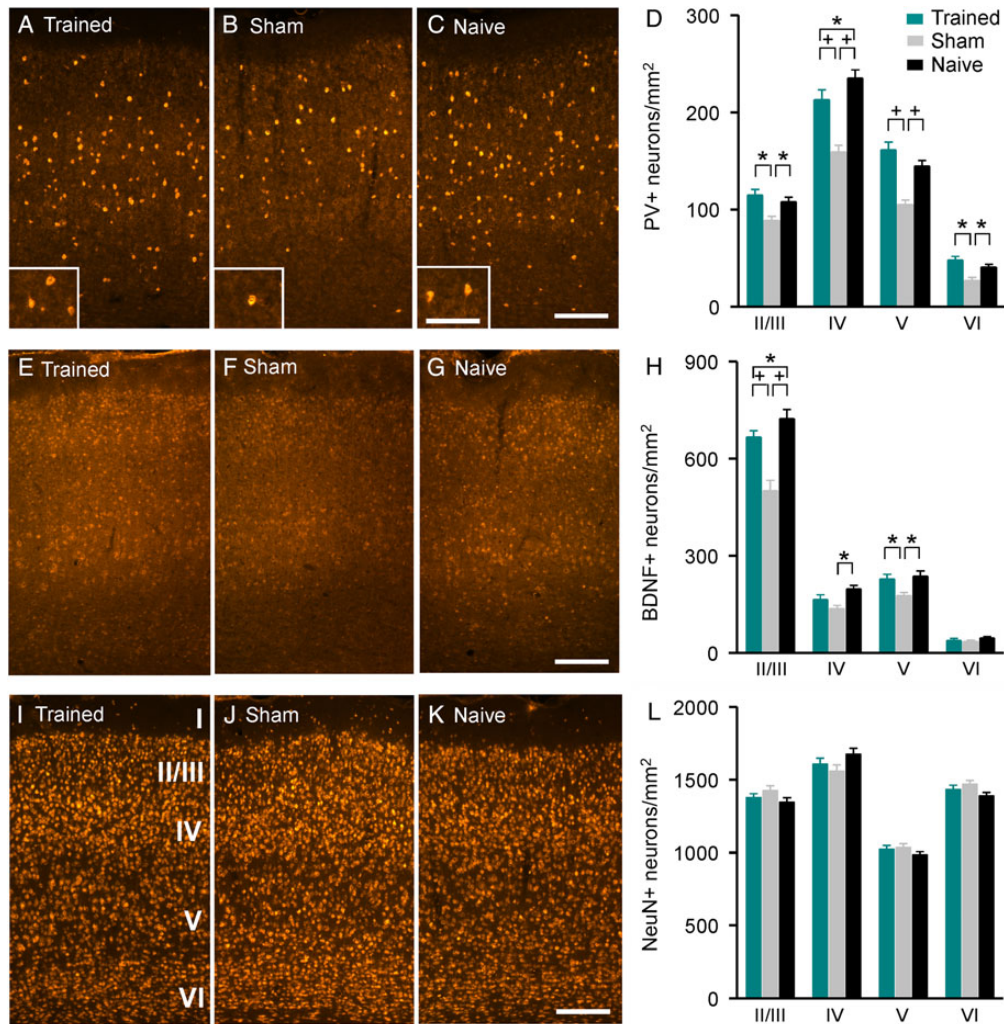
Figure 5. Training-induced recovery in cortical PV and BDNF expressions. (A–C) Photomicrographs of PV+ cortical sections for trained (A), sham (B), and naïve (C) rats. Insets show dendritic PV immunoreactivity in different rat groups. Scale bar presents 200 μm (100 μm in inset). (D) Average PV+ neuron counts for trained (6 hemispheres), sham (6 hemispheres), and naïve (6 hemispheres) rats. Error bars represent SEM. * or +, P < 0.05 or 0.001. (E–G) Photomicrographs of BDNF+ cortical sections for trained (E), sham (F), and naïve (G) rats. Scale bar presents 200 μm. (H) Average BDNF+ neuron counts for trained (6 hemispheres), sham (6 hemispheres), and naïve (6 hemispheres) rats. (I–K) Photomicrographs of NeuN-immunostained cortical sections for trained (I), sham (J), and naïve (K) rats. Cortical layers are indicated in I. Scale bar presents 200 μm. (L) Average NeuN-immunostained neuron counts for trained (6 hemispheres), sham (6 hemispheres), and naïve (6 hemispheres) rats.

and D). Note that PV+ neurons in cortical layer IV of trained rats also increased in number, but still differed from naïve rats (2-way ANOVA with Student–Newman–Keuls post hoc test, $P = 0.006$).

As shown in Figure 5E–H, the number of BDNF-immunostained (BDNF+) neurons was also significantly different across cortical layers (2-way ANOVA, $P < 0.001$) and among the 3 groups ($P < 0.001$). Decreased expressions of BDNF across layers IV–V in sham rats (2-way ANOVA with Student–Newman–Keuls post hoc test, both $P < 0.05$) were again reversed following behavioral training such that the number of BDNF+ neurons in trained rats was now comparable with those in naïve rats (2-way ANOVA with Student–Newman–Keuls post hoc test, both $P > 0.16$). BDNF + neurons in cortical layer II/III of trained rats also increased but still differed from naïve rats (2-way ANOVA with Student–Newman–Keuls post hoc test, $P = 0.013$). It should be noted that cortical neuron densities shown by NeuN staining did not differ for the 3 groups (2-way ANOVA, $P = 0.498$; Fig. 5I–L).

Since NMDA receptor subunit NR2a and NR2b have been implicated in various aspect of developmental and learning-based cortical plasticity (Sun et al. 2005; He et al. 2006; Zhang et al. 2013a,b; Zhu et al. 2014), we quantified cortical protein expressions of NR2a and NR2b for the different rat groups by quantitative immunoblottting (Fig. 6A). As shown in Figure 6B, expression levels of both subunits were significantly lower in sham compared with naïve rats (one-way ANOVA with Student–Newman–Keuls post hoc test, $P < 0.05–0.001$). The percent decreases for NR2a and NR2b versus that of naïve rats were 48.1% and 26.1%, respectively. Therefore, the ratio of NR2a/2b for sham rats also significantly decreased compared with naïve rats (Fig. 6C; one-way ANOVA with Student–Newman–Keuls post hoc test, $P < 0.05$). Training increased down-regulated expressions of both subunits such that the level of NR2b was comparable with that of naïve rats (Fig. 6B; one-way ANOVA with Student–Newman–Keuls post hoc test, $P = 0.12$). Although the expression level of NR2a was still lower than that of naïve rats after training (Fig. 6B; one-way ANOVA with Student–Newman–Keuls post hoc test, $P < 0.05$), the NR2a/2b ratio was reversed (Fig. 6C; one-way ANOVA with Student–Newman–Keuls post hoc test, $P = 0.73$).
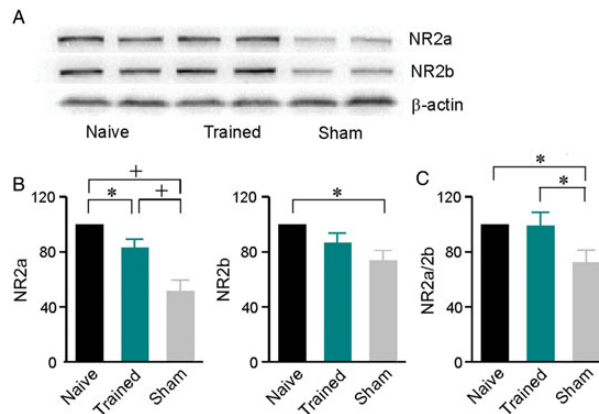
Figure 6. Posttraining effects on cortical expressions of NMDA receptor subunits NR2a and NR2b measured by using the quantitative immunoblotting. (A) Representative Western blots for naïve, trained, and sham rats. (B) Expression levels of NR2a (left) and NR2b (right) subunits. N = 7 for both subunits of all groups of rats. Error bars represent SEM. * or +, P < 0.05 or 0.001. (C) The NR2a/2b ratio for different groups.

Discussion

In this study, we evaluated the possible consequences of low-level lead exposure during development on behavioral and neuronal processing of stimulus repetition-rates in the rodent model. Our exposure protocol resulted in enhanced blood lead level of 7.9–8.2 µg/dL between p9 and p21, a critical period window for auditory cortical development of the rat (Zhang et al. 2002; Insanally et al. 2009, 2010). We found that rats that had lead exposure—even measured after the exposure was stopped and their blood lead concentrations had returned to control values—showed a significant behavioral impairment when conducting an acoustic temporal rate discrimination task. Lead exposure also resulted in a degradation of auditory cortical temporal processing manifested by a reduced spike rate-following ability and by decreased cortical response synchronization. These results demonstrate a neurotoxic impact of low-level lead exposure on cortical auditory processing and auditory-related perceptual ability, particularly in the temporal response domain. Epidemiological studies have reported adverse behavioral and cognitive outcomes in children with similarly low blood lead levels that are not considered lead-poisoned in accordance with the WHO's current screening guidelines (Lanphear et al. 2000; Canfield et al. 2003; Lidsky and Schneider 2003; Braun et al. 2006; Surkan et al. 2007). Although it is still an open question whether rats are more susceptible to lead exposure compared with humans, all these findings recorded in animals and humans emphasize the need for further reduction of the environmental lead exposure in our society (Surkan et al. 2007; Bellinger 2008; Fortune and Lurie 2009; Prins et al. 2010; Zhang et al. 2013a,b).

In addition to functional changes, we also observed alterations in cellular aspects of the cortical machinery. We found decreases in both PV- and BDNF-labeled cortical neurons as a result of early low-level lead exposure. PV+ cortical neurons are believed to be involved in shaping sensory receptive fields and modulating neuronal response properties such as response synchronization and firing timing precision (Gao et al. 2000; de Villers-Sidani et al. 2008, 2010; Desgent et al. 2010; Zhou and Merzenich 2012; Moore and Wehr 2013). A recent study has shown, for example, that cortical PV+ neurons have markedly faster response latencies and are well tuned for frequency, indicating their critical roles in regulating the temporal precision of cortical responses instead of shaping frequency tuning (Moore and Wehr 2013). Less precise coding of repetitive stimuli also has been

reported previously in the aged auditory cortex characterized by fewer PV+ neurons with simplified dendritic arborizations (de Villers-Sidani et al. 2010). In addition, BDNF also is an enabler of cortical growth and plasticity; an interaction between cortical BDNF and GABAergic inhibition has recently been shown to regulate ocular dominance plasticity in adult visual cortex (Maya Vetencourt et al. 2008; Baroncelli et al. 2010) and has been associated with local response correlation (Maffei 2002). This is consistent with our observation that decreased BDNF expression in lead-exposed animals was paralleled by weaker-than-normal local cortical network coupling in the current study. Thus, decreased cortical PV and BDNF expressions plausibly both contribute to the changes in temporal response fidelity recorded here, following lead exposure. This hypothesis is further strengthened by positive changes in cortical PV and BDNF immunoreactivities after intensive behavioral training, which parallels to the recovery of cortical temporal processing.

NMDA receptors, particularly the subunits NR2a and NR2b, have been shown to play a major role in developmental and training-induced plasticity in the sensory cortex (Sun et al. 2005; He et al. 2006; Yashiro and Philpot 2008; Zhou et al. 2011; Zhang et al. 2013a,b; Zhu et al. 2014). For example, dark-rearing during adulthood altered the NR2a/2b ratio and reactivated ocular dominance plasticity in the visual cortex (He et al. 2006). In the auditory cortex, sound discrimination training increased the NR2a/2b ratio to refine the cortical representation of sound azimuths (Zhang et al. 2013a,b). We observed here a larger decrease in the expression level for NR2a than for NR2b, and thus a decreased NR2a/2b ratio in A1 as a consequence of developmental lead exposure. The following perceptual training, however, nearly restored to normal these lead-induced changes in both absolute and relative expressions of NR2a and NR2b. It should be noted that recent studies have demonstrated that a mouse model exhibiting knockout (KO) of a dyslexia risk gene, Dcdc2, shows abnormal spike-timing precision in the somatosensory cortex as measured in a slice preparation (Che et al. 2014). These mice also display impaired auditory temporal processing at a behavioral level (Truong et al. 2014). Interestingly, these findings have been attributed to synaptic hyperexcitability reflecting enhanced NR2b since bath applying the NR2b-specific blocker Ro 25-6981 restores temporal precision in KO neurons (Che et al. 2014). All these results thus indicate that both up- and/or down-regulation of NR2a/2b at the cortical synapse can plausibly

degrade timing precision (and hence temporal encoding). Behavioral training applied in this study may remediate cortical temporal fidelity by restoring the proper expression profile of certain neurotransmitter receptors, like those containing NR2a or NR2b. The development of cortical temporal processing depends on regulated expression of these neurotransmitter receptors (Flint et al. 1997; Roberts and Ramoa 1999); early low-level lead exposure may disrupt the normal development of temporal processing by interfering with expressions of these receptors.

Low-level lead is a risk factor for cognitive and behavioral deficits in children including attention deficit hyperactivity disorder, dyslexia, and other learning disabilities (Lidsky and Schneider 2003; Braun et al. 2006; Surkan et al. 2007; Zhang et al. 2013a,b; Grandjean and Landrigan 2014). These clinical indications are associated with deficits in auditory temporal processing (Wright et al. 1997; Nagarajan et al. 1999; Ahissar et al. 2001; Fitch and Tallal 2003; Paterson et al. 2006; Fitch et al. 2013). To date, the neurological bases of these low-level lead-induced behavioral deficits have not been determined. Importantly, lead-exposed children have been found to be deficient in various aspects of auditory temporal processing; such deficits impact not only speech reception abilities but also associated cognitive and learning abilities (Wright et al. 1997; Nagarajan et al. 1999). These studies thus suggest a clear disturbing association between low-level lead exposure, deficits in auditory temporal processing, and behavioral dysfunction. The fact that low-level lead exposure results in deficits in rapid successive-signal processing and local network coordination in A1 supports the idea that these recorded cortical deficits may account for at least part of the reduced performance acuity for lead-exposed rats while conducting behavioral tasks. At the same time, we do note, with certainty, that recorded changes in PV+ inhibitory neurons, BDNF+ neurons, and NMDA receptor subunits are on a scale that they likely contribute to the expression of neurological and behavioral deficits.

We mainly focused on the auditory cortex while investigating the neural bases underlying the adverse effects of low-level lead exposure on rat's behavioral ability. It remains to be determined whether these observed cortical deficits also occur in other cortical fields. Indeed, earlier studies have shown that postnatal exposure to lead which produces blood lead levels of ~20–30 μg/dL (i.e., ~3 folds higher than that measured in the present study) impairs the development of columnar processing units in rat barrel field cortex (Wilson et al. 2000, 2011). It is also important to remember that reduced performing acuity for lead-exposed rats cannot be attributed to changes at the cortical level alone; subcortical deficits are likely also contributing to deficit expression (Jones et al. 2008). Furthermore, it has been shown that temporal acoustic processing deficits recorded in rats exposed prenatally to the antimitotic teratogen methylazoxymethanol acetate are accompanied by malformations in cortical development (Threlkeld et al. 2009). Here we did not see any changes in size or body weight of rats after low-level lead exposure, indicating the lead doses used in this study can be considered subtoxic. While we do notice reduced dentritic PV immunoreactivity for these lead-exposed animals, their neuron density in each cortical layer as shown by NeuN staining remains intact. It is interesting to further examine cortical morphological consequences of low-level lead exposure as applied in this study. Finally, earlier studies have shown that pentobarbital anesthesia can affect cortical responses to successive stimuli (Lu et al. 2001; Liang et al. 2002). However, anesthesia would not create a bias while measuring cortical temporal responses and their changes in this study because identical anesthetic conditions were applied during recording for all animal cohorts.

Chelation therapy, which aims to reduce the blood lead level, continues to be the primary means of treating lead-poisoned children. However, recent studies demonstrate that this protocol has no significant impact in reversing lead-induced behavioral or cognitive deficits in children because neurotoxic effects persist even after the cessation of the exposure and the blood lead level returns to a normal level (Murphy and Regan 1999; Rogan et al. 2001; Lidsky and Schneider 2003; Bellinger 2008). Thus, the challenge remains of how to devise new, more efficacious intervention strategies to ameliorate these neurotoxic effects induced by previous low-level lead exposure.

Many studies support the idea that experience-dependent plasticity of the auditory system (particularly A1) continues into adulthood (Weinberger 2004; Sanes and Bao 2009; Carcea and Froemke 2013; Schreiner and Polley 2014). Acoustic inputs in conjunction with behavioral training or with stimulation of the basal forebrain or vagus nerve induce persistent auditory cortical changes in the mature brain (Recanzone et al. 1993; Kilgard and Merzenich 1998; Engineer et al. 2011, 2014; David et al. 2012). Our earlier studies have demonstrated that it is possible to restore the developmentally degraded neuronal response dynamics in the adult auditory cortex by using appropriate forms of intensive behavioral training (Zhou and Merzenich 2007, 2009; Guo et al. 2012). Here we extended these findings from prior research by showing that a modified discrimination task applied for ~50 days almost completely reverses the lead-induced deficits in temporal processing and promotes recovery of some related molecular expressions in the cortical field A1. The refinement in cortical representation of stimuli achieved through intensive training has been proposed to facilitate more accurate encoding of acoustic inputs, thereby improving behavioral outcomes (Zhou and Merzenich 2009). Indeed, reducing the central acoustic temporal integration threshold by adaptive computer training has been demonstrated to significantly improve speech and language comprehension abilities of children (Merzenich et al. 1996). To the best of our knowledge, our studies present the first demonstration that intensive training promotes recovery from deficits in auditory temporal response fidelity resulting from low-level lead exposure even after they have occurred. These results suggest a new direction for ameliorating the devastating effects of developmental lead exposure on children. Further study of the underlying mechanisms would be of great practical and theoretical importance for the treatment of childhood lead intoxication.

Supplementary Material

Supplementary material can be found at: http://www.cercor. oxfordjournals.org/.

Funding

Notes

References

Ahissar E, Nagarajan S, Ahissar M, Protopapas A, Mahncke H, Merzenich MM. 2001. Speech comprehension is correlated with temporal response patterns recorded from auditory cortex. Proc Natl Acad Sci USA. 98:13367–13372.

Bao S, Chang EF, Davis JD, Gobeske KT, Merzenich MM. 2003. Progressive degradation and subsequent refinement of acoustic representations in the adult auditory cortex. J Neurosci. 23:10765–10775.

Bao S, Chang EF, Woods J, Merzenich MM. 2004. Temporal plasticity in the primary auditory cortex induced by operant perceptual learning. Nat Neurosci. 7:974–981.

Baroncelli L, Sale A, Viegi A, Maya Vetencourt JF, De Pasquale R, Baldini S, Maffei L. 2010. Experience-dependent reactivation of ocular dominance plasticity in the adult visual cortex. Exp Neurol. 226:100–109.

Bellinger DC. 2008. Lead neurotoxicity and socioeconomic status: conceptual and analytical issues. Neurotoxicology. 29:828–832.

Bowen GP, Lin D, Taylor MK, Ison JR. 2003. Auditory cortex lesions in the rat impair both temporal acuity and noise increment thresholds, revealing a common neural substrate. Cereb Cortex. 13:815–822.

Braun JM, Kahn RS, Froehlich T, Auinger P, Lanphear BP. 2006. Exposures to environmental toxicants and attention deficit hyperactivity disorder in U.S. children. Environ Health Perspect. 114:1904–1909.

Brosch M, Schreiner CE. 1999. Correlations between neural discharges are related to receptive field properties in cat primary auditory cortex. Eur J Neurosci. 11:3517–3530.

Cai R, Zhou X, Guo F, Xu J, Zhang J, Sun X. 2010. Maintenance of enriched environment-induced changes of auditory spatial sensitivity and expression of GABAA, NMDA, and AMPA receptor subunits in rat auditory cortex. Neurobiol Learn Mem. 94:452–460.

Canfield RL, Henderson CR Jr, Cory-Slechta DA, Cox C, Jusko TA, Lanphear BP. 2003. Intellectual impairment in children with blood lead concentrations below 10 microg per deciliter. N Engl J Med. 348:1517–1526.

Carcea I, Froemke RC. 2013. Cortical plasticity, excitatory-inhibitory balance, and sensory perception. Prog Brain Res. 207:65–90.

Che A, Girgenti MJ, LoTurco J. 2014. The dyslexia-associated gene dcdc2 is required for spike-timing precision in mouse neocortex. Biol Psychiatry. 76:387–396.

David SV, Fritz JB, Shamma SA. 2012. Task reward structure shapes rapid receptive field plasticity in auditory cortex. Proc Natl Acad Sci USA. 109:2144–2149.

Desgent S, Boire D, Ptito M. 2010. Altered expression of parvalbumin and calbindin in interneurons within the primary visual cortex of neonatal enucleated hamsters. Neuroscience. 171:1326–1340.

de Villers-Sidani E, Alzghoul L, Zhou X, Simpson KL, Lin RC, Merzenich MM. 2010. Recovery of functional and structural age-related changes in the rat primary auditory cortex with operant training. Proc Natl Acad Sci USA. 107:13900–13905.

de Villers-Sidani E, Simpson KL, Lu YF, Lin RC, Merzenich MM. 2008. Manipulating critical period closure across different sectors of the primary auditory cortex. Nat Neurosci. 11:957–965.

Dietrich KN, Succop PA, Berger OG, Keith RW. 1992. Lead exposure and the central auditory processing abilities and cognitive development of urban children: the Cincinnati Lead Study cohort at age 5 years. Neurotoxicol Teratol. 14:51–56.

Eggermont JJ. 1992. Neural interaction in cat primary auditory cortex. Dependence on recording depth, electrode separation, and age. J Neurophysiol. 68:1216–1228.

Engineer CT, Perez CA, Carraway RS, Chang KQ, Roland JL, Kilgard MP. 2014. Speech training alters tone frequency tuning in rat primary auditory cortex. Behav Brain Res. 258:166–178.

Engineer ND, Riley JR, Seale JD, Vrana WA, Shetake JA, Sudanagunta SP, Borland MS, Kilgard MP. 2011. Reversing pathological neural activity using targeted plasticity. Nature. 470:101–104.

Fitch RH, Alexander ML, Threlkeld SW. 2013. Early neural disruption and auditory processing outcomes in rodent models: implications for developmental language disability. Front Syst Neurosci. 7:58.

Fitch RH, Tallal P. 2003. Neural mechanisms of language-based learning impairments: insights from human populations and animal models. Behav Cogn Neurosci Rev. 2:155–178.

Flint AC, Maisch US, Weishaupt JH, Kriegstein AR, Monyer H. 1997. NR2A subunit expression shortens NMDA receptor synaptic currents in developing neocortex. J Neurosci. 17:2469–2476.

Fortune T, Lurie DI. 2009. Chronic low-level lead exposure affects the monoaminergic system in the mouse superior olivary complex. J Comp Neurol. 513:542–558.

Gao WJ, Wormington AB, Newman DE, Pallas SL. 2000. Development of inhibitory circuitry in visual and auditory cortex of postnatal ferrets: immunocytochemical localization of calbindin- and parvalbumin-containing neurons. J Comp Neurol. 422:140–157.

Grandjean P, Landrigan PJ. 2014. Neurobehavioural effects of developmental toxicity. Lancet Neurol. 13:330–338.

Guo F, Zhang J, Zhu X, Cai R, Zhou X, Sun X. 2012. Auditory discrimination training rescues developmentally degraded directional selectivity and restores mature expression of GABAA and AMPA receptor subunits in rat auditory cortex. Behav Brain Res. 229:301–307.

Han YK, Köver H, Insanally MN, Semerdjian JH, Bao S. 2007. Early experience impairs perceptual discrimination. Nat Neurosci. 10:1191–1197.

He HY, Hodos W, Quinlan EM. 2006. Visual deprivation reactivates rapid ocular dominance plasticity in adult visual cortex. J Neurosci. 26:2951–2955.

Insanally MN, Albanna BF, Bao S. 2010. Pulsed noise experience disrupts complex sound representations. J Neurophysiol. 103:2611–2617.

Insanally MN, Kover H, Kim H, Bao S. 2009. Feature-dependent sensitive periods in the development of complex sound representation. J Neurosci. 29:5456–5462.

Jones LG, Prins J, Park S, Walton JP, Luebke AE, Lurie DI. 2008. Lead exposure during development results in increased neurofilament phosphorylation, neuritic beading, and temporal processing deficits within the murine auditory brainstem. J Comp Neurol. 506:1003–1017.

Kilgard MP, Merzenich MM. 1998. Plasticity of temporal information processing in the primary auditory cortex. Nat Neurosci. 1:727–731.

Lanphear BP, Dietrich K, Auinger P, Cox C. 2000. Cognitive deficits associated with blood lead concentrations 10 microg/dL in US children and adolescents. Public Health Rep. 115:521–529.

Liang L, Lu T, Wang X. 2002. Neural representations of sinusoidal amplitude and frequency modulations in the primary auditory cortex of awake primates. J Neurophysiol. 87:2237–2261.

Lidsky TI, Schneider JS. 2003. Lead neurotoxicity in children: basic mechanisms and clinical correlates. Brain. 126:5–19.

Lu T, Liang L, Wang X. 2001. Temporal and rate representations of time-varying signals in the auditory cortex of awake primates. Nat Neurosci. 4:1131–1138.

Maffei L. 2002. Plasticity in the visual system: role of neurotrophins and electrical activity. Arch Ital Biol. 140:341–346.

Maya Vetencourt JF, Sale A, Viegi A, Baroncelli L, De Pasquale R, O'Leary OF, Castrén E, Maffei L. 2008. The antidepressant fluoxetine restores plasticity in the adult visual cortex. Science. 320:385–388.

Merzenich MM, Jenkins WM, Johnston P, Schreiner C, Miller SL, Tallal P. 1996. Temporal processing deficits of language-learning impaired children ameliorated by training. Science. 271:77–81.

Moore AK, Wehr M. 2013. Parvalbumin-expressing inhibitory interneurons in auditory cortex are well-tuned for frequency. J Neurosci. 33:13713–13723.

Murphy KJ, Regan CM. 1999. Low-level lead exposure in the early postnatal period results in persisting neuroplastic deficits associated with memory consolidation. J Neurochem. 72:2099–2104.

Nagarajan S, Mahncke H, Salz T, Tallal P, Roberts T, Merzenich MM. 1999. Cortical auditory signal processing in poor readers. Proc Natl Acad Sci USA. 96:6483–6488.

Paterson SJ, Heim S, Friedman JT, Choudhury N, Benasich AA. 2006. Development of structure and function in the infant brain: implications for cognition, language and social behaviour. Neurosci Biobehav Rev. 30:1087–1105.

Polley DB, Read HL, Storace DA, Merzenich MM. 2007. Multiparametric auditory receptive field organization across five cortical fields in the albino rat. J Neurophysiol. 97:3621–3638.

Polley DB, Steinberg EE, Merzenich MM. 2006. Perceptual learning directs auditory cortical map reorganization through top-down influences. J Neurosci. 26:4970–4982.

Prins JM, Brooks DM, Thompson CM, Lurie DI. 2010. Chronic low-level Pb exposure during development decreases the expression of the voltage-dependent anion channel in auditory neurons of the brainstem. Neurotoxicology. 31:662–673.

Profant O, Burianová J, Syka J. 2013. The response properties of neurons in different fields of the auditory cortex in the rat. Hear Res. 296:51–59.

Recanzone GH, Schreiner CE, Merzenich MM. 1993. Plasticity in the frequency representation of primary auditory cortex following discrimination training in adult owl monkeys. J Neurosci. 13:87–103.

Roberts EB, Ramoa AS. 1999. Enhanced NR2A subunit expression and decreased NMDA receptor decay time at the onset of ocular dominance plasticity in the ferret. J Neurophysiol. 81:2587–2591.

Rogan WJ, Dietrich KN, Ware JH, Dockery DW, Salganik M, Radcliffe J, Jones RL, Ragan NB, Chisolm JJ Jr, Rhoads GG, Treatment of Lead-Exposed Children Trial Group. 2001. The effect of chelation therapy with succimer on neuropsychological development in children exposed to lead. New Engl J Med. 344:1421–1426.

Rothenberg SJ, Poblano A, Schnaas L. 2000. Brainstem auditory evoked response at five years and prenatal and postnatal blood lead. Neurotoxicol Teratol. 22:503–510.

Rybalko N, Suta D, Popelár J, Syka J. 2010. Inactivation of the left auditory cortex impairs temporal discrimination in the rat. Behav Brain Res. 209:123–130.

Sanes DH, Bao S. 2009. Tuning up the developing auditory CNS. Curr Opin Neurobiol. 19:188–199.

Schreiner CE, Polley DB. 2014. Auditory map plasticity: diversity in causes and consequences. Curr Opin Neurobiol. 24:143–156.

Singer W, Panford-Walsh R, Knipper M. 2014. The function of BDNF in the adult auditory system. Neuropharmacology. 76:719–728.

Sun W, Mercado E 3rd, Wang P, Shan X, Lee TC, Salvi RJ. 2005. Changes in NMDA receptor expression in auditory cortex after learning. Neurosci Lett. 374:63–68.

Surkan PJ, Zhang A, Trachtenberg F, Daniel DB, McKinlay S, Bellinger DC. 2007. Neuropsychological function in children with blood lead levels <10 microg/dL. Neurotoxicology. 28:1170–1177.

Threlkeld SW, Hill CA, Cleary CE, Truong DT, Rosen GD, Fitch RH. 2009. Developmental learning impairments in a rodent model of nodular heterotopia. J Neurodev Disord. 1:237–250.

Truong DT, Che A, Rendall AR, Szalkowski CE, LoTurco JJ, Galaburda AM, Fitch RH. 2014. Mutation of Dcdc2 in mice leads to impairments in auditory processing and memory ability. Genes Brain Behav. doi: 10.1111/gbb.12170.

van Rossum MC. 2001. A novel spike distance. Neural Comput. 13:751–763.

Weinberger NM. 2004. Specific long-term memory traces in primary auditory cortex. Nat Rev Neurosci. 5:279–290.

WHO. 1995. Inorganic Lead. Environmental Health Criteria 165. International Programme on Chemical Safety. Geneva: WHO.

Wilson MA, Johnston MV, Goldstein GW, Blue ME. 2000. Neonatal lead exposure impairs development of rodent barrel field cortex. Proc Natl Acad Sci USA. 97:5540–5545.

Wilson MA, Pedramfard M, Carr PD, Harinarayan N, Johnston MV, Blue ME. 2011. Effect of lead exposure on dendritic spine development in rodent barrel cortex. Program No. 231.07. 2011 Neuroscience Meeting Planner. Washington, DC: Society for Neuroscience, 2011. Online.

Wright BA, Lombardino LJ, King WM, Puranik CS, Leonard CM, Merzenich MM. 1997. Deficits in auditory temporal and spectral resolution in language-impaired children. Nature. 387:176–178.

Yashiro K, Philpot BD. 2008. Regulation of NMDA receptor subunit expression and its implications for LTD, LTP, and metaplasticity. Neuropharmacology. 55:1081–1094.

Zhang LI, Bao S, Merzenich MM. 2002. Disruption of primary auditory cortex by synchronous auditory inputs during a critical period. Proc Natl Acad Sci USA. 99:2309–2314.

Zhang N, Baker HW, Tufts M, Raymond RE, Salihu H, Elliott MR. 2013a. Early childhood lead exposure and academic achievement: evidence from Detroit public schools, 2008–2010. Am J Public Health. 103:e72–e77.

Zhang Y, Zhao Y, Zhu X, Sun X, Zhou X. 2013b. Refining cortical representation of sound azimuths by auditory discrimination training. J Neurosci. 33:9693–9698.

Zhou X, Merzenich MM. 2009. Developmentally degraded cortical temporal processing restored by training. Nat Neurosci. 12:26–28.

Zhou X, Merzenich MM. 2012. Environmental noise exposure degrades normal listening processes. Nat Commun. 3:843 doi:10.1038/ncomms1849.

Zhou X, Merzenich MM. 2007. Intensive training in adults refines A1 representations degraded in an early postnatal critical period. Proc Natl Acad Sci USA. 104:15935–15940.

Zhou X, Panizzutti R, de Villers-Sidani E, Madeira C, Merzenich MM. 2011. Natural restoration of critical period plasticity in the juvenile and adult primary auditory cortex. J Neurosci. 31:5625–5634.

Zhu X, Wang F, Hu H, Sun X, Kilgard MP, Merzenich MM, Zhou X. 2014. Environmental acoustic enrichment promotes recovery from developmentally degraded auditory cortical processing. J Neurosci. 34:5406–5415.